

# Decarboxylation of carbonyloxy radicals: a density functional study†

Matthias Kling‡ and Stefan Schmatz\*

Institut für Physikalische Chemie, Universität Göttingen, Tammannstrasse 6, 37077 Göttingen, Germany. E-mail: ssschmat@gwdg.de

Received 24th April 2003, Accepted 18th July 2003

First published as an Advance Article on the web 5th August 2003

We present a thorough theoretical investigation on the decarboxylation process of carbonyloxy radicals of general structure  $RC(O)O$  which play a key role in the decomposition of organic peroxides that are widely used as initiators in free-radical polymerizations. The effect of variation in the molecular structure ( $R = PhO$ ,  $PhCH_2$  and  $NphO$ ) ( $Nph = naphthyl$ ) is studied systematically. Geometries, energies, and vibrational frequencies of the carbonyloxy radicals, the dissociation products, and the first-order saddle points pertinent to decarboxylation have been calculated employing density functional theory. The results are compared with recent data for the benzoyloxy radical ( $R = Ph$ ). Insertion of an oxygen atom or a  $CH_2$  group between the chromophore and the  $CO_2$  moiety yields a significant reduction in the stability of the carbonyloxy radicals. Despite the structural similarity of the three compounds, the reaction coordinates are markedly different. The structural effects are discussed in terms of changes in thermochemistry, barrier heights and transition modes. The calculated data serve as essential input parameters for statistical unimolecular rate theory calculations and are crucial for the modeling of recent femtosecond pump/probe spectroscopy experiments on the carbonyloxy radical decomposition mechanism.

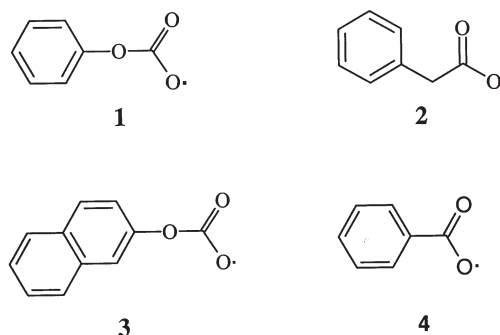
## 1. Introduction

Large organic peroxides are molecules not only of strong fundamental, but also of considerable industrial interest due to their widespread use as initiators in free-radical polymerizations.<sup>1–4</sup> The decomposition of peroxides of type  $RC(O)O-O-tert-butyl$  with  $R$  being an aryl compound<sup>5–8</sup> into the three species  $R^\bullet$ ,  $tert-butyl$  and  $CO_2$  can in principle occur *via* a concerted or a stepwise mechanism. It is now accepted that the latter mechanism is the rule in  $RC(O)O-O-tert-butyl$  decay so that intermediate carbonyloxy radicals,  $RCO_2^\bullet$ , that are formed after  $O-O$  bond fission play a key role in this process. The carbonyloxy radical might subsequently decarboxylate to form  $CO_2$  and the radical  $R$ . Investigations on substituted aryloxy radicals in solution yield lifetimes in the nanosecond to microsecond range,<sup>7,9,10</sup> which allow these intermediates to escape the solvent cage and initiate the polymerization. Shorter (ps) lifetimes have been attributed to 9-methylfluorenylcarbonyloxy,<sup>11</sup> benzylcarbonyloxy and benzoyloxy radicals.<sup>12,13</sup> The time scale of the decarboxylation of carbonyloxy intermediates strongly determines the initial polymerization steps and is crucial for the efficiency of the whole polymerization process.<sup>4,14</sup> It is thus an important issue to fully understand the decomposition mechanism and to study the detailed dynamics of these systems.

A large body of papers on thermally induced peroxide decomposition has been accumulated over the years, and photochemically induced studies have been carried out on the microsecond to nanosecond time scale. Only recently, Abel *et al.* have used femtosecond pump/probe-spectroscopy to gain a much more detailed insight into the decomposition

mechanism.<sup>7,8,10</sup> In a combination of different spectroscopic techniques and theoretical modelling a meaningful picture of the energy-dependent decarboxylation dynamics of naphthoyloxy<sup>7</sup> and benzoyloxy radicals<sup>10</sup> was obtained. The model is based on statistical unimolecular rate theory in conjunction with a master equation formalism to account for vibrational energy transfer of the initially hot species. Crucial input parameters are reaction barrier heights and vibrational frequencies of the reactants and the intermediate carbonyloxy radicals. Using these quantities as obtained from density functional theory (DFT) calculations, experimental concentration *vs.* time profiles could be quantitatively simulated. The next step is to study the influence of molecular structure, *i.e.* variation of the residue  $R$ , on the fragmentation dynamics and kinetics. This is the key feature in controlling efficiencies. So far, the dependence of the dynamics on structure and internal energy is not fully understood due to the lack of *systematic* theoretical and experimental studies.<sup>4,14</sup>

In this work, we study the influence of intermediate carbonyloxy radical structure on the decarboxylation kinetics and present DFT calculations on the decarboxylation of carbonyloxy radicals  $RCO_2^\bullet$  with  $R = PhO$  (**1**),  $PhCH_2$  (**2**) and  $NphO$



Scheme 1

† Electronic supplementary information (ESI) available: Tables 3–5: Harmonic vibrational frequencies  $\omega_i$  of the reactant and the saddle point species for  $RC(O)O$  ( $R = PhO$ ,  $PhCH_2$  and  $NphO$ ). See <http://www.rsc.org/suppdata/cp/b3/b304544g/>

‡ Current address: UC Berkeley, Department of Chemistry, Hildebrand D90, Berkeley, CA 94720, USA.

(3) (Scheme 1). We compare the results with recent data obtained for the benzoyloxy radical ( $R = \text{Ph}$ ) (**4**),<sup>10</sup> which is also shown in Scheme 1. In order to study the structural dependence in a systematic way, we first insert an oxygen atom between the  $\text{CO}_2$  unit and the ring, yielding **1**. Substituting in this species (a) the bridging oxygen atom by a  $\text{CH}_2$  group (there are thus two hydrogen atoms instead of the lone electron pairs) and (b) the chromophore by the larger naphthyl (Nph) residue, we obtain **2** and **3**, respectively.

The calculated values are important input parameters for the simulation of experimental data based on the previously proposed model for the decomposition of organic peroxides and the decarboxylation of carbonyloxy radicals.<sup>10</sup> The experimental data and a detailed presentation of the modeling can be found elsewhere.<sup>8</sup> Here, we focus on a comparative description of the characteristics of the potential energy surfaces (PESs) for the decarboxylation of carbonyloxy radicals. The changes in thermochemistry, barrier heights, and transition modes with carbonyloxy radical structure are discussed.

The paper is organized as follows: in Section 2, we describe the methodology while Section 3 reports on the results for the three radicals and a comparison with benzoyloxy. Section 4 contains our conclusions.

## 2. Methodology

As in our previous work on the benzoyloxy radical,<sup>10</sup> DFT calculations on geometries and energies for the phenyloxy-carbonyloxy ( $\text{PhO}-\text{CO}_2$ ), benzylcarbonyloxy ( $\text{PhCH}_2-\text{CO}_2$ ), and naphthyloxy-carbonyloxy ( $\text{NphO}-\text{CO}_2$ ) radicals were performed for isolated molecules. However, the results should be applicable to molecules embedded in an environment of nonpolar and perhaps even of weakly polar aprotic solvent molecules as employed in our spectroscopic experiments.<sup>7,8,10</sup> To our best knowledge, no quantum chemical calculations on the three radicals have been reported so far.

In the present work, geometry optimizations were carried out with the DFT variant UB3LYP<sup>15–17</sup> that employs Becke's 3-parameter nonlocal exchange functional<sup>18</sup> and the nonlocal correlation functional of Lee, Yang and Parr.<sup>19</sup> The 6-31G(d), 6-311+G(d,p), 6-311+G(2d,p) and 6-311+(2df,2pd) basis sets are used in our calculations. They comprise 160, 250, 300 and 410 contracted Gaussian-type orbitals (cGTOs), respectively, for  $\text{PhO}-\text{CO}_2$ ; 164, 262, 312 and 438 cGTOs for  $\text{PhCH}_2-\text{CO}_2$ ; and 224, 350, 420 and 574 cGTOs for  $\text{NphO}-\text{CO}_2$ . The GAUSSIAN98<sup>20</sup> package was used in all of the DFT calculations reported in this work.

The structures of the relevant stationary points (reactants, products, and first-order saddle points pertinent to decarboxylation) on the PESs of the three radicals first were fully optimized at the UB3LYP/6-31G(d) level of theory and then refined using the 6-311+G(d,p) basis set. To confirm that true minima on the PES have been found, the Hessian matrices at the stationary points were calculated. The energies were further corrected for zero-point vibrational effects (at the harmonic level; imaginary frequencies not included). The TS routine of GAUSSIAN98 and the intrinsic reaction coordinate (IRC) method<sup>21,22</sup> were employed for the calculation of the transition state (first-order saddle point) geometries. At the UB3LYP/6-311+G(d,p) optimized geometries, single-point calculations with the 6-311+G(2d,p) and 6-311+G(2df,2pd) basis sets were performed (Table 1).

In our previous work on the benzoyloxy radical,<sup>10</sup> large-scale *ab initio* calculations were reported that made use of partially restricted coupled cluster theory (variant RCCSD(T)) based on a restricted Hartree–Fock determinant in conjunction with a flexible basis set of 347 cGTOs. The three most sensitive geometrical parameters  $r_1(\text{C}-\text{C})$ ,  $r_2(\text{C}-\text{O})$  and  $\alpha(\text{O}-\text{C}-\text{O})$  of the benzoyloxy radical have been optimized, and the differ-

**Table 1** Relative energies (in  $\text{kcal mol}^{-1}$ ) of reactants and first order saddle point structures for decarboxylation<sup>a</sup>

	Basis set	$E_{\text{el}}$	$E_0$
$\text{PhO}-\text{CO}_2$	6-311+G(d,p)	2.3	1.3 <sup>c</sup>
	6-311+G(2df,2pd) <sup>b</sup>	3.2	2.2 <sup>c</sup>
$\text{PhCH}_2-\text{CO}_2$	6-311+G(d,p)	2.6	1.5 <sup>c</sup>
	6-311+G(2df,2pd) <sup>b</sup>	2.2	1.1 <sup>c</sup>
$\text{NphO}-\text{CO}_2$	6-311+G(2d,p)	0.06	-0.5 <sup>c</sup>
	6-311+G(2df,2pd) <sup>d</sup>	0.05	-0.5 <sup>c</sup>

<sup>a</sup> The energy of the reactant is set to zero for all reactions and basis sets used in the calculations.  $E_{\text{el}}$  denotes the electronic energies, while  $E_0$  includes corrections due to zero point vibrational effects (at the harmonic level). Absolute energy values in Hartree and results for the other basis sets reported in Section 2 are available from the authors upon request. <sup>b</sup> Calculated at the UB3LYP/6-311+G(d,p) geometries.

<sup>c</sup> ZPE calculated employing 6-311+G(d,p) basis set. <sup>d</sup> Calculated at the UB3LYP/6-311+G(2d,p) geometry. <sup>e</sup> ZPE calculated employing 6-311+G(2d,p) basis set.

ences between the optimum RCCSD(T) geometrical parameters and those obtained by UB3LYP/6-311+G(d,p) were in the order of 0.001 Å and 1°, respectively. From these results we expect that the UB3LYP geometries are also very close to the corresponding large-scale coupled cluster values for the radicals studied in the present work. A further comparison between UB3LYP data for the benzoyloxy radical and results obtained employing the UB3PW91 correlation functional of Perdew and Wang<sup>23,24</sup> showed that the differences are negligible. The DFT calculations<sup>10</sup> yielded a physically reasonable saddle point structure with an appropriate transition mode. Employing the corresponding barrier height in statistical rate-theory calculations, we obtained a very good agreement with the experimental data. We are thus confident that the UB3LYP results for three similar aryloxy-carbonyloxy and benzylcarbonyloxy radicals reported in the present work may serve as reliable input data for simulations based on statistical rate theories.

It is well-known that unrestricted single-determinant wave functions (such as unrestricted Hartree–Fock, UHF) exhibit a large spin contamination in aryl and benzyl radicals.<sup>25,26</sup> Although such a contamination from higher-spin excited states would certainly affect the molecular geometries and the energetics, it was shown that spin contamination in unrestricted density functional calculations is usually small (no spin contamination would occur in DFT calculations if the exact functionals were known).<sup>27–29</sup> Hybrid density functionals such as B3LYP have a somewhat higher spin contamination due to the admixture of Hartree–Fock exchange. In all our calculations, the deviation of the average  $\langle S^2 \rangle$  values from the eigenvalues  $S(S+1) = 0.75$  does not exceed 5% so that spin contamination does not affect our results.

## 3. Results and discussion

Due to the flatness of the PESs in the vicinity of the first order saddle points pertinent to decarboxylation, the search for the geometries of these saddle points for the phenyloxy-carbonyloxy, benzylcarbonyloxy and naphthyloxy-carbonyloxy radicals turned out to be quite complicated. On the contrary, in the case of the benzoyloxy radical the geometry optimization was much less time-consuming due to the highly symmetric saddle point structure.<sup>10</sup> The results from our UB3LYP calculations are contained in Tables 1–5. Relative energies of reactants and transition states are summarized in Table 1, while reaction enthalpies are given in Table 2. Harmonic vibrational frequencies  $\omega_i$  of the reactant and the saddle point species are reported in Tables 3–5 (ESI†).

**Table 2** Relative energies (in kcal mol<sup>-1</sup>) of reactants and products for decarboxylation<sup>a</sup>

	$E_{\text{el}}^b$	$E_{\text{el}}^c$	$E_0^c$	$\Delta_{\text{R}}H^\circ(298 \text{ K})^c$
PhO-CO <sub>2</sub>	-30.9	-29.7	-31.2	-30.8
PhCH <sub>2</sub> -CO <sub>2</sub>	-27.4	-28.3	-30.3	-29.9
NphO-CO <sub>2</sub>	-31.7	-30.6	-31.5	-31.2

<sup>a</sup> The energy of the reactant is set to zero for all reactions.  $E_{\text{el}}$  denotes the electronic energies, while  $E_0$  includes corrections due to zero point vibrational effects (at the harmonic level). Also given in the table is the standard enthalpy of reaction  $\Delta_{\text{R}}H^\circ(298 \text{ K})$ . Absolute energy values in Hartree are available from the authors upon request. <sup>b</sup> UB3LYP/6-311+G(d,p). <sup>c</sup> UB3LYP/6-311+G(2df,2pd) at UB3LYP/6-311+G(d,p) geometries; ZPE and thermal corrections for 298 K are calculated employing 6-311+G(d,p) basis set.

### 3.1 Phenoxycarbonyloxy radical (PhO-CO<sub>2</sub>)

The PhO-CO<sub>2</sub> radical belongs to point group  $C_1$ . The oxygen atom of the CO<sub>2</sub> group that points towards the ring is termed the inner oxygen atom whereas the other oxygen is termed the outer atom. The geometry according to our UB3LYP/6-311+G(d,p) calculations is graphically displayed in Fig. 1. The carboxylic C-O bonds in the radical are calculated to be 1.248 Å (outer) and 1.250 Å (inner). The Ph-O-CO<sub>2</sub> angle is calculated to be 117.1°, while the torsional angle between the carbon atom of the CO<sub>2</sub> group and the ring plane amounts to 68.1°.

In the saddle point structure pertinent to decarboxylation (Fig. 1), the Ph-O bond distance has become slightly shorter by 0.029 Å whereas the O-CO<sub>2</sub> distance is elongated by 0.041 Å. The outer C-O bond has become larger (1.252 Å) whereas the inner CO bond has been shortened to 1.225 Å. The Ph-O-CO<sub>2</sub> angle in the saddle point structure measures 122.8° and the CO<sub>2</sub> group is tilted out of the ring plane by only 32.2°. In summary, the transition state is very close to the reactant structure (“early” transition state). Note that the two O-C-C angles in the ring differ by about 10°: While the angle at the side where the CO<sub>2</sub> group is located is calculated to be 124.3°, the other O-C-C angle measures only 114.4°. The  $C_{2v}$ -symmetric product phenyloxy radical exhibits a Ph-O bond distance of 1.253 Å (UB3LYP/6-311+G(d,p)).

The transition mode corresponding to decarboxylation is described as follows (Fig. 2): The Ph-O bond is shortened, whereas the O-CO<sub>2</sub> bond is considerably stretched and eventually broken. Simultaneously, the CO<sub>2</sub> group becomes coplanar with the phenyl ring and attains a linear configuration. The motion is governed by the outer oxygen atom of the CO<sub>2</sub> group, whereas the displacement vectors of the other two oxygen atoms and the carboxylic carbon atom are considerably smaller.

In the case of the decarboxylation of the benzylcarbonyloxy radical (see Section 3.2), the CH<sub>2</sub>-CO<sub>2</sub>  $\sigma$ -bond is almost perpendicular to the ring plane (see Fig. 5). This implicates that

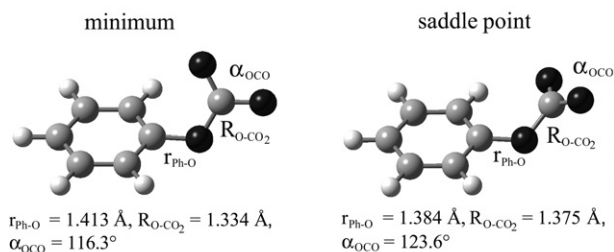


**Fig. 1** Optimized geometries of the phenoxycarbonyloxy radical and the saddle point leading to decarboxylation (UB3LYP/6-311+G(d,p) results).

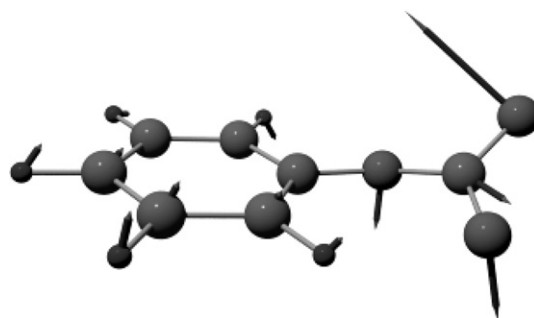


**Fig. 2** Representation of the normal mode  $Q_{\text{TS}}$  with imaginary frequency  $\omega_{\text{TS}} = 147i \text{ cm}^{-1}$  (transition mode) at the saddle point for decarboxylation of the phenoxycarbonyloxy radical. For details see the text.

after dissociation the unpaired electron is located in a  $\pi$ -type orbital and the product benzyl radical in its  $^2B_1$  electronic ground state is formed.<sup>30</sup> For the phenoxycarbonyloxy radical, however, from Fig. 2 it could be anticipated that breaking the  $\sigma$ -bond leaves the unpaired electron in a  $\sigma$ -type orbital in the ring plane, comparable to the situation of the decarboxylation of the benzoyloxy radical where a phenyl radical in its  $^2A_1$  electronic ground state was produced.<sup>10</sup>

From experimental and theoretical work it is known<sup>31-35</sup> that the electronic ground state of the phenoxy radical is  $^2B_1$  with a  $\pi$ -type SOMO. Liu *et al.* reported UNO-CAS/6-31G\* calculations without inclusion of the in-plane lone electron pair at oxygen,<sup>31</sup> and in a subsequent paper<sup>33</sup> these calculations were extended to 9 electrons in 8 orbitals including the in-plane lone pair. The CASSCF geometry for the electronic ground state shows very good agreement with our B3LYP results. The lowest  $n \rightarrow \pi$  transition yields the  $1^2B_2$  excited state at 30.2 kcal mol<sup>-1</sup> above the electronic ground state (state-averaged CASSCF calculation<sup>31</sup>). Takahashi *et al.* calculated the excitation energy  $X^2B_1 \rightarrow 1^2B_2$  to be 36.3 kcal mol<sup>-1</sup> (CASSCF/DZV + MRSD-CI).<sup>32</sup> This state may be identified with the first excited state at  $(24.4 \pm 1.2)$  kcal mol<sup>-1</sup> observed by Lineberger and co-workers by means of UV photoelectron spectroscopy.<sup>35</sup> Thus, the corresponding  $\sigma$ -radical is accessible at the relevant energies in our experiment.<sup>8</sup> In this species, the C-O bond (1.352 Å, UMP2/6-31G\*<sup>33</sup>) is considerably longer than in the ground state (1.225 Å at UMP2/6-31G\* 1.258 Å at B3LYP/6-31G\*<sup>33</sup> in good agreement with our result) and thus close to a typical C-O single bond. The ring exhibits a regular hexagonal structure while in the electronic ground state a quinoidal structure is found.

In contrast to the expectation from inspection of Fig. 2, the clear result of our intrinsic reaction coordinate (IRC) calculations is that the first order saddle point described above correlates with the  $^2B_1$  ground state of the phenoxy radical (see Fig. 3). Note that the final energy in Fig. 3 is below PhO ( $^2B_1$ ) + CO<sub>2</sub> ( $1^1\Sigma_g^+$ ) due to the long-range electrostatic attraction between the fragments (see Section 3.5). The IRC calculations give clear evidence that the electronic reorganization during the decarboxylation process is more complex than should be expected from simple MO-considerations.

The barrier height was calculated from single point calculations at the UB3LYP/6-31G(d) and UB3LYP/6-311+G(d,p) geometries. The differences with respect to basis set convergence are relatively small. While triple-zeta quality of the basis set and the addition of diffuse functions increase the barrier by 0.9 kcal mol<sup>-1</sup>, further polarization functions (f functions at the heavy nuclei and d functions at hydrogen nuclei) result only in a slight change of the barrier height. We recommend  $E_0 = 2.2 \text{ kcal mol}^{-1}$  for the zero-point energy corrected barrier.

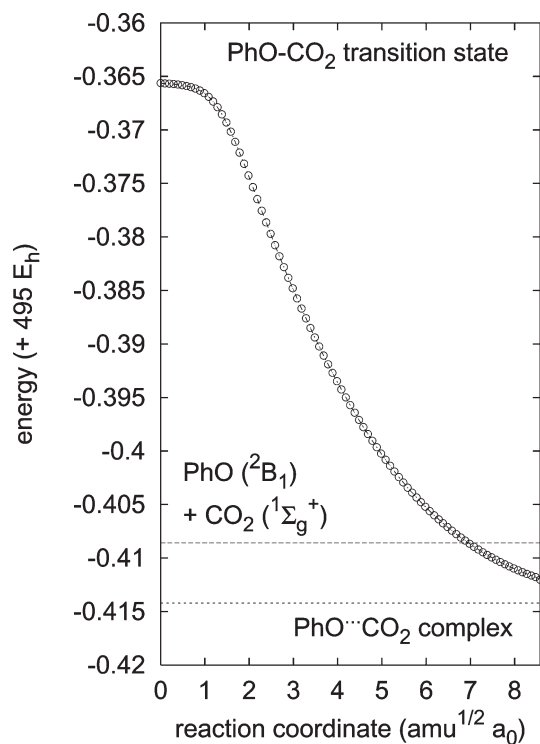


Fig. 3 Potential energy along the intrinsic reaction coordinate for the decarboxylation process  $\text{PhO-CO}_2 \rightarrow \text{PhO} + \text{CO}_2$ .

### 3.2 Benzylcarbonyloxy radical ( $\text{PhCH}_2\text{-CO}_2$ )

A similar situation is encountered for the  $\text{PhCH}_2\text{-CO}_2$  species ( $C_1$  symmetry). According to our UB3LYP/6-311+G(d,p) calculations, the geometry of this radical in its electronic ground state is described as follows (Fig. 4): Both hydrogen atoms of the methylene group ( $\text{H-C-H}$  bond angle  $\alpha = 106.4^\circ$ ) are located on the same side of the ring, one of them being almost coplanar with it (torsional angle  $16.7^\circ$ ). The  $\text{Ph-CH}_2$  and the  $\text{CH}_2\text{-CO}_2$  bond distances are almost equal. The carboxylic carbon atom is tilted out of the phenyl ring plane by a torsional angle of  $74.2^\circ$ . The torsional angle between the  $\text{CO}_2$  group and the plane orthogonal to the ring plane through the  $\text{Ph-CH}_2$  bond is calculated to be  $13.9^\circ$ . The bond between the carboxylic carbon atom and the (inner) oxygen atom that points towards the ring is  $1.262 \text{ \AA}$ , whereas the bond to the other (outer) oxygen atom amounts to  $1.251 \text{ \AA}$ .

In the saddle point species pertinent to decarboxylation (Fig. 4), the  $\text{Ph-CH}_2$  distance is slightly shortened, while the dissociating  $\text{CH}_2\text{-CO}_2$  bond is stretched by  $0.044 \text{ \AA}$ . The two CO distances amount to  $1.223 \text{ \AA}$  (inner) and  $1.291 \text{ \AA}$  (outer). The  $\text{Ph-CH}_2\text{-CO}_2$  angle has become slightly smaller from  $112.1$  to  $110.6^\circ$  in the transition state while the carboxylic carbon atom is tilted out of the ring plane by  $67.3^\circ$  in the saddle point species, thus almost unchanged with respect to the reactant. The torsional angle between the  $\text{CO}_2$  group and the

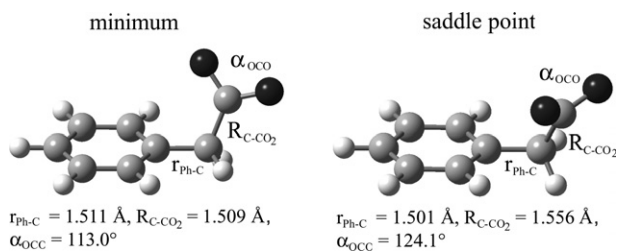


Fig. 4 Optimized geometries of the benzylcarbonyloxy radical and the saddle point leading to decarboxylation (UB3LYP/6-311+G(d,p) results).

plane orthogonal to the ring plane through the  $\text{Ph-CH}_2$  bond has become considerably larger ( $44.2^\circ$ ). The inner hydrogen atom of the  $\text{CH}_2$  group is still almost coplanar with the phenyl ring (with a torsional angle of  $11.6^\circ$ ). In summary, the saddle point structure is geometrically very close to that of the reactant species. This corresponds to a characterization as an “early” transition state. The  $C_{2v}$ -symmetric product benzyl radical exhibits a  $\text{Ph-CH}_2$  bond distance of  $1.405 \text{ \AA}$  with a methylene group characterized by  $r(\text{C-H}) = 1.083 \text{ \AA}$  and  $\alpha(\text{H-C-H}) = 117.7^\circ$  (UB3LYP/6-311+G(d,p)).

The transition mode (see Fig. 5) is described by a normal coordinate that is markedly different from the case of the  $\text{PhO-CO}_2$  species. Here, the reactive normal coordinate  $Q_{\text{TS}}$  is described as a stretching of the  $\text{CH}_2\text{-CO}_2$  bond and a simultaneous widening of the  $\text{CO}_2$  angle. The  $\text{PhCH}_2$  skeleton is only little affected by the reactive normal mode. The  $\text{CH}_2$  group rotates into the ring plane towards the symmetric product structure of the benzyl radical (see Fig. 5). Note that the displacement vector of the carbon atom in the  $\text{CO}_2$  group dominates  $Q_{\text{TS}}$ .

The barrier height for decarboxylation of  $\text{PhCH}_2\text{-CO}_2$  is about one half of the corresponding value for  $\text{PhO-CO}_2$ , and the basis set convergence behavior is different: While a basis set of triple-zeta quality with an additional set of diffuse functions results only in a small change of the barrier height,  $f$  functions at the heavy atoms yield a decrease of the barrier height  $E_0$  by  $0.7 \text{ kcal mol}^{-1}$ . We obtain a zero-point energy corrected barrier height of  $1.07 \text{ kcal mol}^{-1}$ .

### 3.3 Naphthylcarbonyloxy radical ( $\text{NphO-CO}_2$ )

The naphthylcarbonyloxy radical in its electronic ground state should be very similar to the  $\text{PhO-CO}_2$  structure. Our UB3LYP/6-31G(d) calculations for the naphthylcarbonyloxy radical yield a very small barrier to decarboxylation of  $0.7 \text{ kcal mol}^{-1}$ . Since this value is particularly sensitive to small changes in the geometry, the single point calculations at the UB3LYP/6-31G(d) geometry with the 6-311+G(2d,p) and 6-311+G(2df,2pd) basis sets yield *negative* values for the barrier height which do not have any physical significance. As a consequence, we optimized the geometry employing the larger basis set 6-311+G(2d,p). The result is that the barrier becomes even smaller and almost negligible. If the harmonic zero-point vibrational energy is added to the classical potential, the effective (or adiabatic) barrier is again lower than zero. However, the harmonic zero-point energy is a crucial quantity due to large anharmonicity effects in particular in the intermolecular modes. In order to obtain a reliable value for the height of the barrier to decarboxylation in  $\text{NphO-CO}_2$ , high-level quantum dynamical calculations have to be performed which are out of reach for us at present.

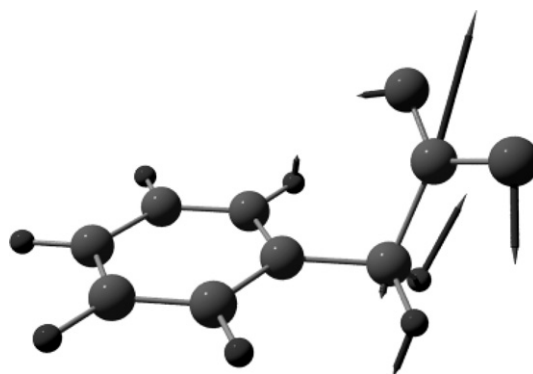


Fig. 5 Representation of the normal mode  $Q_{\text{TS}}$  with imaginary frequency  $\omega_{\text{TS}} = 795i \text{ cm}^{-1}$  (transition mode) at the saddle point for decarboxylation of the benzylcarbonyloxy radical. For details see the text.

The analysis of the results reveals that the UB3LYP/6-311+G(2d,p) geometry (Fig. 6) differs markedly from the PhO-CO<sub>2</sub> structure (UB3LYP/6-311+G(d,p)): The Nph-O bond is shorter than the O-CO<sub>2</sub> distance, whereas the Nph-O-CO<sub>2</sub> angle  $\alpha = 113.7^\circ$  is only  $3^\circ$  smaller than in PhO-CO<sub>2</sub>. The outer C-O bond is calculated to be 1.210 Å whereas the inner one is longer by 0.044 Å. The O-C-O angle in the CO<sub>2</sub> moiety is almost  $10^\circ$  larger than in PhO-CO<sub>2</sub>. The low reaction barrier corresponds with the characterization of the transition state as “early”. Most of the geometrical parameters in the saddle point structure (Fig. 6) are only very slightly changed with respect to the reactant species ( $r(\text{C-O})_{\text{inner}} = 1.210$  Å,  $r(\text{C-O})_{\text{outer}} = 1.250$  Å,  $\alpha(\text{Nph-O-CO}_2) = 114.1^\circ$ ). At the saddle point,  $r(\text{Nph-O})$  is shortened by 0.023 Å and  $r(\text{O-CO}_2)$  is elongated by 0.053 Å. The torsional angle between the carboxylic carbon atom and the naphthyl plane slightly decreases from  $53.4^\circ$  in the reactant species to  $49.1^\circ$  in the saddle point. The Nph-O distance in the C<sub>s</sub>-symmetric product naphthyloxy radical is calculated to be 1.248 Å (UB3LYP/6-311+G(d,p)).

The transition mode (Fig. 7) differs considerably from the PhO-CO<sub>2</sub> counterpart. While in the latter case the outer carboxylic oxygen atom dominated the normal mode, in NphO-CO<sub>2</sub> the motion of the carboxylic carbon atom is most pronounced. The O-CO<sub>2</sub> bond stretches along with a simultaneous widening of the O-C-O angle. The Nph-O bond becomes shorter. In summary, the decarboxylation coordinate is more similar to the case of PhCH<sub>2</sub>-CO<sub>2</sub> than to that of PhO-CO<sub>2</sub>.

### 3.4 Comparison with the benzoyloxy radical (PhCO<sub>2</sub>)

In comparison to the UB3LYP/6-311+G(d,p) results obtained for the benzoyloxy radical,<sup>10</sup> the present three systems show significant differences: the C-O bond distances in benzoyloxy (1.266 Å) are markedly longer, while the O-C-O bond angle is similar, apart from the case NphO-CO<sub>2</sub> where this angle is enlarged by about  $10^\circ$ . The X-CO<sub>2</sub> bond distances are shortest for the two aryloxy carbonyloxy radicals (X = O) and longest for the benzylcarbonyloxy species (X = CH<sub>2</sub>) with its pure  $\sigma$ -type bonding situation; benzoyloxy exhibits an intermediate situation ( $r(\text{C-CO}_2) = 1.472$  Å). While, as discussed above, the three saddle point structures of this work can be classified as “early” transition states, the situation in benzoyloxy is much more shifted to the product side (Ph-CO<sub>2</sub> distance enlarged by as much as 0.40 Å, C-O bond lengths decreased to 1.20 Å, O-C-O angle widened by as much as  $36^\circ$ ). At 8.4 kcal mol<sup>-1</sup>, the barrier for decarboxylation of benzoyloxy is much higher than for the other three radicals. The reason for this behavior may be found in the strong  $\pi$ -electron delocalization in the planar C<sub>2v</sub>-symmetric benzoyloxy system.

### 3.5 Long-range interactions between the fragments

During the search for the saddle points, several other interesting stationary points on the PESs have been identified, in particular complexes formed between linear carbon dioxide

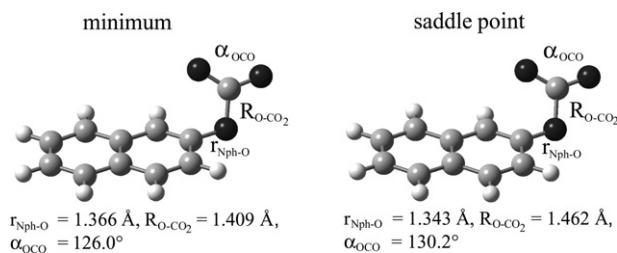


Fig. 6 Optimized geometries of the naphthyloxy carbonyloxy radical and the saddle point leading to decarboxylation (UB3LYP/6-311+G(2d,p) results).

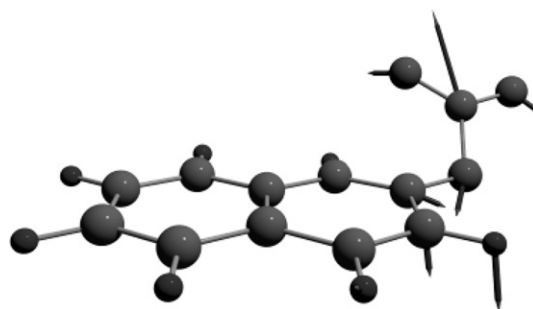


Fig. 7 Representation of the normal mode  $Q_{\text{TS}}$  with imaginary frequency  $\omega_{\text{TS}} = 257i$  cm<sup>-1</sup> (transition mode) at the saddle point for decarboxylation of the naphthyloxy carbonyloxy radical. For details see the text.

and the product species (phenyl, benzyl, phenoxy and naphthyloxy radicals, respectively). These complexes which are mainly due to long-range electrostatic (dipole-quadrupole) interaction should not be relevant for the dissociations, but rather for the reverse association processes.

Considering the association reactions, shallow minima are found which correspond to dipole-quadrupole interactions between CO<sub>2</sub> and the product radicals. However, only the dipole moments of the phenoxy (4.06 D at UB3LYP/6-311+G(d,p) level) and naphthoxy (4.94 D at UB3LYP/6-311+G(2d,p) level) radicals are sufficiently large so that significant wells with classical depths of 3.5 and 3.6 kcal mol<sup>-1</sup>, respectively, occur in the potential energy profile along the reaction coordinate. The minima for the dissociating benzoyloxy and benzylcarbonyloxy systems are very shallow due to the smaller dipole moments of the phenyl (0.78 D) and benzyl (0.15 D) radicals (UB3LYP/6-311+G(d,p)). Note that in all four product radicals the negative end of the dipole moment vector is located at the site of the dissociated CO<sub>2</sub> moiety. In the C<sub>s</sub>-symmetric complexes, the PhO...CO<sub>2</sub> and NphO...CO<sub>2</sub> distances measure 2.835 and 2.819 Å, respectively. All atoms lie in one plane and carbon dioxide attains an almost linear conformation (the deviation from linearity amounts to  $3^\circ$  in all cases discussed here). There are additional saddle points with respect to rotational motion of the CO<sub>2</sub> unit perpendicular to its axis of symmetry and the plane of the complexes. The corresponding barrier heights are calculated to be 0.9 kcal mol<sup>-1</sup> (UB3LYP/6-311+G(d,p)) for both phenoxy and naphthyloxy complexes with intermolecular O-CO<sub>2</sub> distances of 2.814 and 2.804 Å, respectively. Thus the CO<sub>2</sub> unit can rotate freely at energies below the product asymptotic energy.

## 4. Conclusions

The structure dependence of the decarboxylation of carbonyloxy radicals has been studied employing the DFT variant UB3LYP. For the first time, we have presented results for carbonyloxy radicals RCO<sub>2</sub> with R = PhCH<sub>2</sub>, PhO and NphO, which are compared with those obtained recently for the benzoyloxy radical (R = Ph).<sup>10</sup> Very good agreement was found previously for the barrier height of the benzoyloxy radical as calculated by DFT-methods and estimated from experimental data.<sup>10</sup> Benzoyloxy radicals are quite stable towards decarboxylation in their ground-state, quantitatively explaining lifetimes in the ns- $\mu$ s range at ambient temperatures.<sup>6,36</sup> In contrast, benzoyloxy radicals, RCO<sub>2</sub> with R = PhCH<sub>2</sub>, PhO and NphO in their electronic ground state turned out to be much less stable towards decarboxylation. The barrier towards decarboxylation decreases in the order PhCO<sub>2</sub> > PhOCO<sub>2</sub> > PhCH<sub>2</sub>CO<sub>2</sub> > NphOCO<sub>2</sub>.

One reason for this structure dependence as proposed by Bartlett and Hiatt in their pioneering work<sup>37</sup> is a change in

stability of product radicals. Our calculations give an increase in exothermicity of about 30 kcal mol<sup>-1</sup> by going from benzoyloxy to the other carbonyloxy radicals. According to the Bell–Evans–Polanyi principle,<sup>38,39</sup> this trend is accompanied by a corresponding decrease of the reaction barrier height. However, the structure dependence evidently is more complex.

Starting from PhO–CO<sub>2</sub>, one should expect a similar behavior by (a) substituting the bridging oxygen atom by the isolobal methylene group (PhCH<sub>2</sub>–CO<sub>2</sub>) or (b) changing the phenyl by a naphthyl moiety (NphO–CO<sub>2</sub>). However, the decarboxylation reaction coordinates of PhO–CO<sub>2</sub> and PhCH<sub>2</sub>–CO<sub>2</sub> or NphO–CO<sub>2</sub> are markedly different while there is some similarity between the latter two species. The curvature  $k_{TS} = \mu\omega_{TS}^2$  at the saddle point is smallest for PhO–CO<sub>2</sub> (harmonic vibrational frequency of the transition mode  $\omega_{TS} = 147i$  cm<sup>-1</sup>), almost three times as high for NphO–CO<sub>2</sub> (257i cm<sup>-1</sup>) and considerably larger for PhCH<sub>2</sub>–CO<sub>2</sub> (795i cm<sup>-1</sup>). The reduced mass pertinent to decarboxylation is smaller for NphO–CO<sub>2</sub> (11.52 amu) compared to PhO–CO<sub>2</sub> (13.52 amu) while the opposite effect should be expected from simple mass arguments. PhCH<sub>2</sub>–CO<sub>2</sub> exhibits the smallest reduced mass (9.81 amu) which may be rationalized by the role of the hydrogen atoms in this system. In order to get a deeper insight into the reaction dynamics of the decarboxylation processes, classical trajectory calculations and/or quantum dynamical investigations have to be performed on reliable potential energy surfaces. Work in this direction is currently being carried out in our laboratory.

With the electronic energies, barrier heights, and vibrational frequencies of the carbonyloxy radicals, experimental data on the kinetics of the decarboxylation of these radicals can be modeled quantitatively.<sup>10</sup> The order of the decarboxylation rate for carbonyloxy radicals as observed by means of femtosecond absorption spectroscopy is in surprisingly good agreement with model predictions based on our DFT calculations.<sup>8</sup> The absolute barrier heights used in the successful modeling of the experimentally observed thermal decarboxylation of carbonyloxy radicals do usually not differ by more than 2 kcal mol<sup>-1</sup> from our theoretical results. Thus, we consider the accuracy of our DFT calculations to be reasonable for a semi-quantitative understanding of the decarboxylation kinetics in the electronic ground state of carbonyloxy radicals.

The correlation of structure and kinetics is the key feature in controlling chemistry (e.g. initiation efficiency in free-radical polymerization) through substitution. With reliable molecular parameters deduced from DFT calculations, the decarboxylation of carbonyloxy radicals, as produced in the decomposition of organic peroxides, can be modeled quantitatively. This enables us not only to rely on calculations for molecules that have not been synthesized so far, but will also guide us in designing new materials with the desired properties for their use in free-radical polymerization.

## Acknowledgements

The authors wish to thank AKZO Nobel and the Deutsche Forschungsgemeinschaft (Sonderforschungsbereich 357 “Molekulare Mechanismen Unimolekularer Prozesse”) for financial support. We are grateful to Dr R. Oswald for his help with Figs. 3, 5 and 7. Fruitful discussions about various topics of this work with Profs. B. Abel, B. Botschwina, M. Buback, J. Schroeder and J. Troe are gratefully acknowledged.

## References

- 1 K. Fujimori, in *Organic Peroxides*, ed. W. Ando, Wiley, New York, 1992, p. 319.
- 2 Y. Sawaki, in *Organic Peroxides*, ed. W. Ando, Wiley, New York, 1992, p. 425.

- 3 C. A. Barson and J. C. Bevington, *J. Polym. Sci. A: Polym. Chem.*, 1997, **35**, 2955.
- 4 M. Buback and J. Sandmann, *Z. Phys. Chem.*, 2000, **214**, 583.
- 5 J. Chateaufneuf, J. Luszyk and K. U. Ingold, *J. Am. Chem. Soc.*, 1988, **110**, 2877.
- 6 J. Chateaufneuf, J. Luszyk and K. U. Ingold, *J. Am. Chem. Soc.*, 1988, **110**, 2886.
- 7 B. Abel, J. Aßmann, M. Buback, M. Kling, S. Schmatz and J. Schroeder, *Angew. Chem.*, 2003, **115**, 311; B. Abel, J. Aßmann, M. Buback, M. Kling, S. Schmatz and J. Schroeder, *Angew. Chem., Int. Ed.*, 2003, **42**, 299.
- 8 B. Abel, J. Assmann, M. Buback, Ch. Grimm, M. Kling, S. Schmatz, J. Schroeder and T. Witte, *J. Phys. Chem. A*, 2003, in press.
- 9 J. Wang, T. Tateno, H. Sakuragi and K. Tokumaru, *J. Photochem. Photobiol.*, 1995, **92**, 53.
- 10 B. Abel, J. Assmann, P. Botschwina, M. Buback, M. Kling, R. Oswald, S. Schmatz, J. Schroeder and T. Witte, *J. Phys. Chem. A*, 2003, **107**, 5157.
- 11 D. E. Falvey and G. B. Schuster, *J. Am. Chem. Soc.*, 1986, **108**, 7419.
- 12 T. M. Bockman, S. M. Hubig and J. K. Kochi, *J. Am. Chem. Soc.*, 1996, **118**, 4502.
- 13 T. M. Bockman, S. M. Hubig and J. K. Kochi, *J. Org. Chem.*, 1997, **62**, 2210.
- 14 M. Buback, M. Kling, M. T. Seidel, F.-D. Schott, J. Schroeder and U. Steegmüller, *Z. Phys. Chem.*, 2001, **215**, 717.
- 15 A. D. Becke, *J. Chem. Phys.*, 1993, **98**, 1372.
- 16 P. J. Stephens, F. J. Devlin, C. F. Chabalowski and M. J. Frisch, *J. Phys. Chem.*, 1994, **98**, 11623.
- 17 P. J. Stephens, F. J. Devlin, C. S. Ashvar, K. L. Bak, P. R. Taylor and M. J. Frisch, *ACS Symp. Ser.*, 1996, **629**, 105.
- 18 A. D. Becke, *J. Chem. Phys.*, 1993, **98**, 5648.
- 19 C. Lee, W. Yang and R. G. Parr, *Phys. Rev. B*, 1988, **37**, 785.
- 20 M. J. Frisch, G. W. Trucks, H. B. Schlegel, G. E. Scuseria, M. A. Robb, J. R. Cheeseman, V. G. Zakrzewski, J. A. Montgomery, Jr., R. E. Stratmann, J. C. Burant, S. Dapprich, J. M. Millam, A. D. Daniels, K. N. Kudin, M. C. Strain, O. Farkas, J. Tomasi, V. Barone, M. Cossi, R. Cammi, B. Mennucci, C. Pomelli, C. Adamo, S. Clifford, J. Ochterski, G. A. Petersson, P. Y. Ayala, Q. Cui, K. Morokuma, D. K. Malick, A. D. Rabuck, K. Raghavachari, J. B. Foresman, J. Cioslowski, J. V. Ortiz, B. B. Stefanov, G. Liu, A. Liashenko, P. Piskorz, I. Komaromi, R. Gomperts, R. L. Martin, D. J. Fox, T. Keith, M. A. Al-Laham, C. Y. Peng, A. Nanayakkara, C. Gonzalez, M. Challacombe, P. M. W. Gill, B. G. Johnson, W. Chen, M. W. Wong, J. L. Andres, M. Head-Gordon, E. S. Replogle and J. A. Pople, *GAUSS-SIAN 98 (Revision A.9)*, Gaussian, Inc., Pittsburgh, PA, 1998.
- 21 C. Gonzales and H. B. Schlegel, *J. Phys. Chem.*, 1990, **94**, 5523.
- 22 C. Gonzales and H. B. Schlegel, *J. Chem. Phys.*, 1989, **90**, 2154.
- 23 J. P. Perdew, K. Burke and Y. Wang, *Phys. Rev. B*, 1996, **54**, 16533.
- 24 J. P. Perdew, *Electronic Structure of Solids*, ed. P. Ziesche and H. Eschrig, Akademie Verlag, Berlin, 1991.
- 25 J. Cioslowski, G. Liu, M. Martinov, P. Piskorz and D. Moncrief, *J. Am. Chem. Soc.*, 1996, **118**, 5261.
- 26 J. Pacansky, B. Liu and D. DeFrees, *J. Org. Chem.*, 1986, **51**, 3720.
- 27 J. Baker, A. Scheiner and J. Andzelm, *Chem. Phys. Lett.*, 1993, **216**, 380.
- 28 G. J. Laming, N. C. Handy and R. D. Amos, *Mol. Phys.*, 1993, **80**, 1121.
- 29 J. M. Wittbrodt and H. B. Schlegel, *J. Chem. Phys.*, 1996, **105**, 6574.
- 30 R. Janoschek, *Pure Appl. Chem.*, 2001, **73**, 1521; J. E. Rice, N. C. Handy and P. J. Knowles, *J. Chem. Soc., Faraday Trans. 2*, 1987, **83**, 1643. Note: due to different conventions concerning the C<sub>2v</sub> irreducible representations, the electronic ground state is termed <sup>2</sup>B<sub>2</sub>.
- 31 R. Liu and X. Zhou, *J. Phys. Chem.*, 1993, **97**, 9613.
- 32 J. Takahashi, T. Momose and T. Shida, *Bull. Chem. Soc. Jpn.*, 1994, **67**, 964.
- 33 R. Liu, K. Morokuma, A. M. Mebel and M. C. Lin, *J. Phys. Chem.*, 1996, **100**, 9314.
- 34 S. Re and Y. Osamura, *J. Phys. Chem. A*, 1998, **102**, 3798.
- 35 R. F. Gunion, M. K. Gilles, M. L. Polak and W. C. Lineberger, *Int. J. Mass Spectrom. Ion Process.*, 1992, **117**, 601.
- 36 H. Misawa, K. Sawabe, S. Takahara, H. Sakuragi and K. Tokumaru, *Chem. Lett.*, 1988, **23**, 357.
- 37 P. D. Bartlett and R. R. Hiatt, *J. Am. Chem. Soc.*, 1958, **80**, 1398.
- 38 R. P. Bell, *Trans. Faraday Soc.*, 1937, **33**, 496.
- 39 M. G. Evans and M. Polanyi, *Trans. Faraday Soc.*, 1936, **32**, 1333.